

Bone formation and resorption of highly purified β -tricalcium phosphate in the rat femoral condyle

Naoki Kondo^a, Akira Ogose^{a,*}, Kunihiro Tokunaga^a, Tomoyuki Ito^a, Katsumitsu Arai^a, Naoko Kudo^a, Hikaru Inoue^b, Hiroyuki Irie^b, Naoto Endo^a

^a*Division of Orthopedic Surgery, Department of Regenerative and Transplant Medicine, Niigata University Graduate School of Medical and Dental Sciences, 757-1, Asahimachi Dori, Niigata 951-8510, Japan*

^b*Development Department, Olympus Biomaterial Corp., LTD, Tokyo, Japan*

Received 30 November 2004; accepted 14 February 2005

Available online 18 April 2005

Abstract

The aim of this study was to examine the chronological histology associated with highly purified β -tricalcium phosphate (β -TCP) implanted in the rat femoral condyle. Specimens were harvested on days 4, 7, 14, 28 and 56 after implantation, and were analyzed by tartrate-resistant acid phosphatase (TRAP) staining, immunohistochemistry of the ED1 protein as a marker of the phagocyte system, and in situ hybridization with digoxigenin-labeled $\alpha 1$ chain of type I procollagen (COL1A1), osteopontin and osteocalcin. β -TCP was resorbed in a chronological manner. Although new bone was not observed on day 4, fibroblast-like cells around β -TCP were positive for COL1A1 and osteopontin mRNA. New bone formation presented after day 7. In the double-staining for OPN and ED1 on day 7, most cells around β -TCP were positive for either osteopontin mRNA or ED1 protein. However, there were some doubly positive multinucleated cells, suggesting that they belonged to the mononuclear phagocyte system. After day 28, the implanted region was replaced with bone marrow. Multinucleated TRAP-positive and ED1-positive cells which adhered to β -TCP at all stages seemed to be osteoclasts and they continuously resorbed β -TCP. β -TCP has a good biocompatibility since both bioresorption and bone formation started at an early stage after implantation.

© 2005 Elsevier Ltd. All rights reserved.

Keywords: Bioresorption; Calcium phosphate; Macrophage; Osteoblast; Osteoclast

1. Introduction

Various biomaterials have been developed and used as bone graft substitutes for bone defects caused by bone tumors, trauma, and revision total arthroplasty. β -tricalcium phosphate (β -TCP) is a calcium phosphate ceramic that is used as a bone substitute. The biocompatibility and resorption characteristics of β -TCP have been studied [1], but the osteoconductivity of β -TCP has mainly been examined in histological and histomorphometric analyses in vitro [1]. Highly purified β -TCP was

developed in Japan and is now available as a potent bone-grafting substitute for clinical use [2]. Ozawa et al. reported the clinical results of 167 patients who received a highly purified β -TCP implant. None of them developed fractures or deformities [2], and the radiograms showed marked radiological remodeling around β -TCP, because of the good absorbability and osteoconduction of β -TCP [2]. However, few studies have described the detailed histology of the bone tissue response to implanted highly purified β -TCP [1]. In the present study, we analyzed histological and cellular level events occurring around the highly purified β -TCP implanted in the rat femoral condyles by using of histomorphometry, immunohistochemistry, and in situ hybridization.

*Corresponding author. Tel.: 81 25 227 2272; fax: 81 25 227 0782.

E-mail address: aogose@med.niigata-u.ac.jp (A. Ogose).

2. Materials and methods

2.1. Preparation of β -TCP

β -TCP was used by Olympus Biomaterial Co. Ltd. (Tokyo, Japan) [2]. Fine β -TCP powder was synthesized by wet milling (a mechanochemical method). Calcium-deficient hydroxyapatite (CDHA) was obtained by milling dibasic calcium phosphate dihydrate (DCPD) and calcium carbonate (CC) at a molar ratio of 2:1 with pure water and zirconium (Zr) beads, followed by drying at 80 °C. This crystalline solid was converted to β -TCP by calcination at 750 °C for 1 h. Upon sintering of β -TCP powder at 1050 °C for 1 h, a porous β -TCP block was obtained, which was then characterized through assessment of the surface area and pore size distribution of the porous structure. The porosity of the block, as measured by the Archimedes method, was 75% and the surface area, as measured by the Brunauer–Emmett–Teller method, was 1.4 m²/g [3]. The β -TCP block possessed macropores of 100–500 μ m and micropores of less than 5 μ m. Nearly all macropores were interconnected via a 100–200 μ m path. The crushed beads of β -TCP were used in the present study.

2.2. Animal model and tissue preparation

Thirty-five 8-week-old female F344/Fisher rats were used. Under general isoflurane anesthesia, the femoral lateral condyle in each rat was exposed and a hole was drilled in the bone. The width and depth of the hole were both 2 mm. After washing the bone cavity with normal saline to remove debris, the defects of bilateral femora were filled with β -TCP beads up to the preoperative level macroscopically as tightly as possible, and the fascia and skin were then closed. All animal experiments were conducted according to the “Guideline for Animal Experimentation” of OLYMPUS CORPORATION.

On days 4, 7, 14, 28 and 56 after the operation, seven rats were euthanized with diethyl ether. Bilateral femora were removed and immersed in 4% paraformaldehyde (PFA) in 0.1 M phosphate buffer for 5–7 days. The femora were decalcified with 0.5 M EDTA · 2Na solution for 8 days at room temperature and were dehydrated with a graded series of ethanol treatments prior to being embedded in paraffin. Paraffin sections of 4 μ m thickness were cut using a microtome (Leica, Tokyo, Japan) and stored at 4 °C for the following histological evaluations.

2.3. Semi-quantitative evaluation of surface area of β -TCP and the perimeter of new bone formation

Specimens were stained with hematoxylin and eosin (HE). The area of β -TCP was measured using NIH Image Ver.1.63 (developed at the US National Institutes

of Health and available by anonymous FTP, could download as follows; <http://rsb.info.nih.gov/nih-image/download.html>). It was impossible to distinguish between newly formed bone and pre-existing trabeculae in the metaphysis or marrow according to the pattern of HE staining. Therefore, we measured the perimeter of newly formed bone which was directly attached to β -TCP. Statistical analysis was performed by using EXCEL (Microsoft Office 2003) with an unpaired *t*-test, with *p* < 0.05 considered to be a significant difference.

2.4. Tartrate-resistant acid phosphatase (TRAP) staining

To detect osteoclasts, TRAP staining was carried out according to Burstone’s Azo dye method [4], with some modification [5]. Briefly, a mixture of 3 mg of naphthol AS-BI phosphate (Sigma, St. Louis, MO), 18 mg of red violet LB salt (Sigma, St. Louis, MO) and 2.4 mM L(+)-tartaric acid (Wako, Osaka, Japan) diluted in 0.1 M sodium acetate buffer (pH 5.0) were dropped onto the deparaffinized sections. These sections were incubated for 50–60 min at room temperature.

2.5. In situ hybridization

To examine the differentiation stages of bone-forming cells, deparaffinized serial sections from femoral condyles were subjected to mRNA in situ hybridization, as previously described [6,7]. A plasmid containing the 0.49-kb fragment of mouse osteocalcin cDNA was kindly provided by Dr. S. Nomura (Division of Pathology, Department of Pathology and Pathophysiology, Osaka University Graduate School of Medicine, Osaka, Japan). Plasmids containing the 0.5 and 0.37-kb fragments of rat osteopontin and the mouse COL1A1 cDNAs were gifts from the Life Science Research Institute (Asahi-Chemical Industry Co., Shizuoka, Japan). After dewaxing in xylene and rehydrating through a series of graded ethanol treatments, tissue sections were treated with 10 μ g/ml proteinase K (Roche Diagnostics, Mannheim, Germany) for 20 min at 37 °C, refixed with 4% PFA solution, immersed in 0.1 M triethanolamine containing 0.25% acetic acid for 10 min, and washed in 0.1 M phosphate buffer (pH 7.4). The samples were then incubated in a hybridization solution [10 mM Tris-HCl (pH 7.6), 1 mM EDTA (pH 8.0), 600 mM NaCl, 0.25% sodium dodecyl sulfate, 1 × Denhart’s medium, 50% (v/v) deionized formamide/0.5 μ g/ml probe RNA, and 10% dextran sulfate] at 50 °C in a moist chamber for 16 h. Negative controls were incubated with DIG-labeled sense RNA probes. After hybridization, the slides were washed at 55 °C with 50% deionized formamide in 2 × saline-sodium citrate (SSC) (1 × SSC; 0.15 mol/l NaCl, 0.015 mol/l sodium

citrate) for 20 min to remove excess riboprobes. The non-specifically hybridized riboprobes were digested with 10 $\mu\text{g}/\text{ml}$ of RNase A (Roche Diagnostic) solution at 37 °C for 30 min. The specimens were then washed with $2 \times \text{SSC}$ for 15 min and with $0.2 \times \text{SSC}$ for 15 min twice. To visualize the hybridized probe, the slides were incubated with alkaline phosphatase-conjugated anti-DIG antibody (Roche Diagnostics) at room temperature for 60 min after blocking with 1.5% blocking reagent (Roche Diagnostics) in 100 mM Tris-HCl (pH 7.5) for 55 min. The specimens were then washed twice with 100 mM Tris-HCl (pH 7.5) for 15 min, and briefly immersed in 100 mM Tris-HCl (pH 9.5) containing 100 mM NaCl and 50 mM MgCl_2 for 5 min. The colorimetric reaction was performed with nitro blue tetrazolium salt and bromo-4-chloro-3-indolyl phosphate solution (Roche Diagnostics) in the dark for 20–120 min, and then the reaction was stopped with 10 mM Tris-HCl (pH 7.6) containing 1 mM EDTA. Slides were mounted with micro cover glass (Matsunami, Tokyo, Japan) and analyzed under a light microscope with 0.5% methyl green counterstaining.

2.6. Immunohistochemistry for ED1

The anti-ED1 monoclonal antibody recognizes a single chain glycoprotein of MW 90 000–110 000 that is expressed predominantly on the lysosomal membrane and at low levels on the cell surface [8]. ED1 protein is detected in the cells of the mononuclear phagocyte system [9], and its levels of expression and glycosylation are enhanced by phagocytic stimuli [8]. To detect ED1 protein, immunohistochemical analysis was performed. After antigen retrieval with 0.2% trypsin at 37 °C for 20 min, tissue endogenous peroxidases were blocked by treatment with 0.3% H_2O_2 in methanol at room temperature for 10 min, and non-specific reactions were blocked by treatment with 1:10 diluted goat serum (CEDARLANE, Ontario, Canada) at room temperature for 10 min. The sections were incubated with 1:500 diluted anti-ED1 monoclonal antibody (Beringer Mannheim, Augst, Switzerland) for 16 h at 4 °C.

For the immunoreaction, rat MAX-PO (MULTI) secondary antibody (Nichirei, Tokyo, Japan) was used and signals were visualized using a DAB- H_2O_2 substrate (Nichirei, Tokyo, Japan).

2.7. Double staining of osteopontin mRNA and ED1 protein

After in situ hybridization of osteopontin mRNA, we analyzed the distribution of the ED1 protein by immunohistochemistry as described above.

3. Results

β -TCP was recognized as an unstained structure after decalcification. Fig. 1 shows the time course of implanted β -TCP with HE staining. On day 4, there were clots and a considerable number of fibroblast-like cells between the β -TCP beads without newly formed bone (Fig. 1A). By day 7, bone formation occurred in the peripheral region of β -TCP. However, there were still red blood cells and fibroblast-like cells in the central region of the implanted β -TCP (Fig. 1B). On day 14, bone formation was observed in the central region of the implanted β -TCP. Blood vessels were also identified between the beads (Fig. 1C). The area of β -TCP on day 14 was significantly smaller than those on days 4 and 7 ($p < 0.05$) (Fig. 2), and the total perimeter of newly formed bone adhered to β -TCP on day 14 was somewhat longer than that on day 7 (Fig. 3). On day 28, some of the implanted area was replaced with normal bone marrow (Fig. 1D). A semi-quantitative evaluation demonstrated that the area of β -TCP on day 28 was significantly smaller than those on days 4 and 7 ($p < 0.05$) (Fig. 2). The total perimeter of new bone adhered to β -TCP on day 28 was significantly longer than that on day 7 ($p < 0.05$) (Fig. 3). On day 56, much of the implanted area was replaced with normal bone marrow. Most of the β -TCP surface was covered with newly formed bone (Fig. 1E), and the area of β -TCP was significantly smaller than those on days 4, 7 and 14 ($p < 0.05$) (Fig. 2). The total perimeter on day 56 was similar to that on day 28 (Fig. 3).

Immunohistochemistry of the ED1 protein showed the presence of ED1-positive cells around β -TCP at all stages. On day 4, most of the ED1-positive cells were mononuclear cells located around the β -TCP and between the β -TCP beads. Although there were some multinucleated ED1-positive cells around the β -TCP, the number of these cells was much lower than that of the ED1-positive mononuclear cells (Fig. 4A). After day 7, multinucleated ED1-positive cells became dominant around β -TCP and multinucleated giant cells were detected around β -TCP on day 14 (Figs. 4B–D). Furthermore, some TRAP-positive multinucleated cells around β -TCP were also positive for ED1 in the serial sections. In particular, these doubly positive cells were observed on day 4, at a very early stage (Figs. 5A and B). On day 14, TRAP-positive cells increased compared with day 4.

Fig. 6 shows in situ hybridization of COL1A1 mRNA. On day 4, COL1A1 mRNA-positive cells adhered to β -TCP (Fig. 6A) and were also expressed by fibroblast-like cells between the β -TCP beads. On days 7 and 14, COL1A1 mRNA-positive cells adhered to β -TCP and also were aligned with newly formed bone (Fig. 6B). The number of COL1A1 mRNA-positive cells around β -TCP was lower than that around new bone

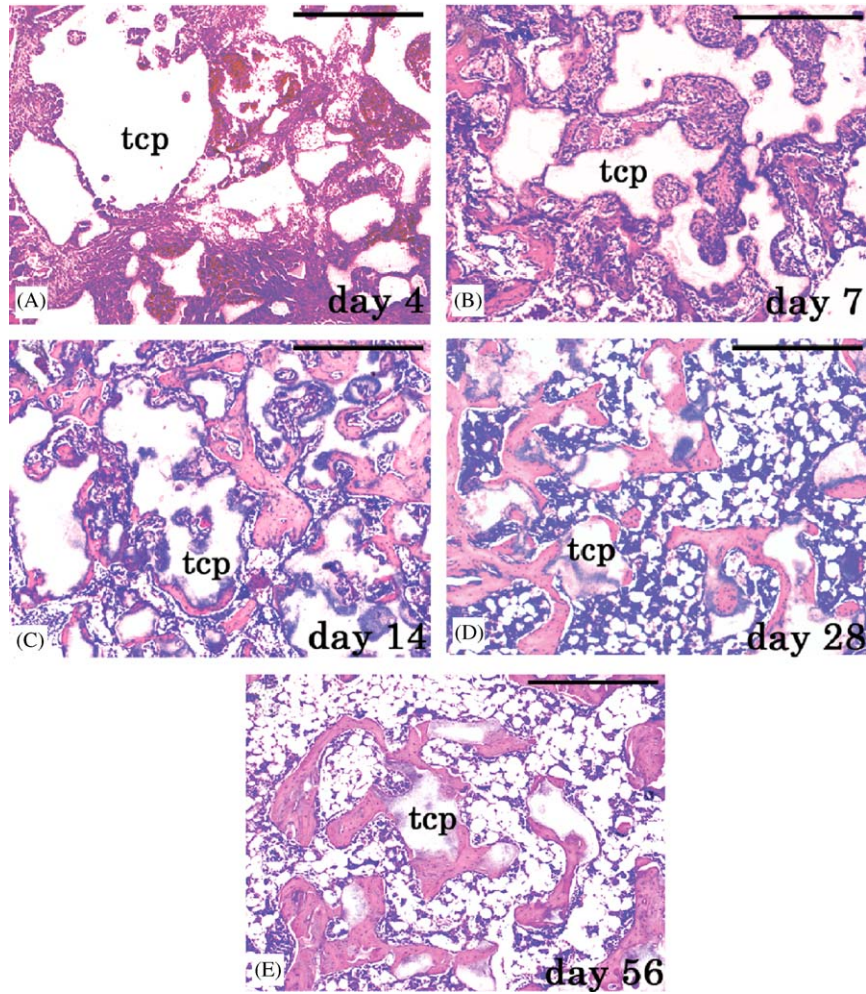


Fig. 1. HE staining **A.** Day 4: There were considerable clots between the β -TCP particles, without new bone formation. Fibroblastic cells, multinucleated cells, and monocytes were observed in the peripheral region of β -TCP. **B.** Day 7: Bone formation occurred in the peripheral region of β -TCP. However, the central region of β -TCP was occupied with fibroblast-like cells and red blood cells without new bone formation. **C.** Day 14: Bone formation also occurred in the central region, and there were many blood vessels between the β -TCP particles. **D.** Day 28: The region of the β -TCP implant was replaced with bone marrow, and the β -TCP area decreased in comparison with the earlier stages. **E.** Day 56: Most of the implanted β -TCP was replaced by bone marrow, and the amount of bone formation declined. tcp, tricalcium phosphate; Bar; A–E, 500 μ m.

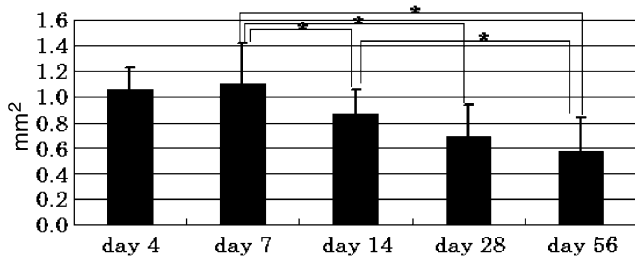


Fig. 2. Area of β -TCP. Each value was shown as mean \pm standard deviation (mm^2). The values were $1.06 \pm 0.17 \text{mm}^2$ on day 4, $1.11 \pm 0.32 \text{mm}^2$ on day 7, $0.87 \pm 0.19 \text{mm}^2$ on day 14, $0.70 \pm 0.24 \text{mm}^2$ on day 28, and $0.57 \pm 0.27 \text{mm}^2$ on day 56. The areas of β -TCP on days 14, 28, and 56 were significantly lower than that on day 7 ($p < 0.05$). *, $p < 0.05$; Bar, standard deviation.

(Fig. 6B). All the COL1A1 mRNA-positive cells were aligned with newly formed bone on day 28 though there were no COL1A1 mRNA-positive cells around β -TCP (Fig. 6C). Similar results were observed on day 56 (Fig. 6D).

Fig. 7 shows in situ hybridization of osteopontin mRNA. The expression of osteopontin mRNA around β -TCP was identified on days 4, 7, 14 and 28, but the signals were negative on day 56 (Fig. 7). Osteopontin mRNA-positive cells around β -TCP were consisted of two types; mononuclear and multinucleated cells. Around newly formed bone, osteopontin mRNA-positive cells were detected on days 7, 14 and 28, but not on day 56. On days 7, 14 and 28, the number of osteopontin

mRNA-positive cells around β -TCP was much higher than that around the newly formed bone (Figs. 7B and C).

The expression of osteocalcin mRNA was only detected on some osteoblasts around the newly formed bone on day 28, and the number of these cells was low (Fig. 8). The expression of osteocalcin mRNA was not detected on the cells around either β -TCP or newly formed bone on days 4, 7, 14 and 56 (data not shown).

The double staining using in situ hybridization of osteopontin mRNA and immunohistochemistry of ED1 showed that most of the cells were single positive for

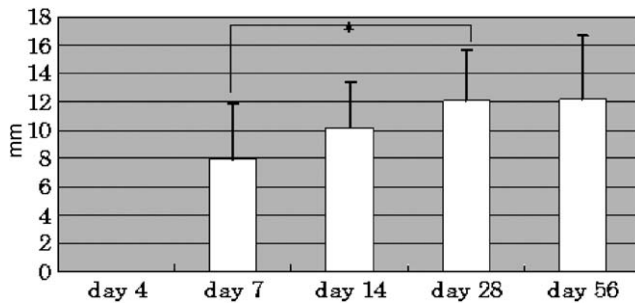


Fig. 3. The perimeter length of the newly formed bone adhered to β -TCP. Each value was shown as mean \pm standard deviation (mm). The values were 7.98 ± 3.96 mm on day 7, 10.1 ± 3.33 mm on day 14, 12.1 ± 3.55 mm on day 28, and 12.2 ± 4.43 mm on day 56. The perimeter length increased in a chronological manner, and the perimeter on day 28 was significantly longer than that on day 7 ($p < 0.05$). *, $p < 0.05$; Bar, standard deviation.

osteopontin mRNA or ED1 on day 7 (Fig. 9). However, some cells were positive for osteopontin mRNA, as well as ED1 (Fig. 9). There was no doubly positive mononuclear cell. Similar results were observed on day 4.

4. Discussion

In the present study, the areas of implanted β -TCP on days 14, 28 and 56 were significantly lower than those on days 4 and 7. This finding indicates that highly purified β -TCP is resorbed in a chronological manner. Chazono et al. also showed that the area of β -TCP implanted in rabbit bone defects decreased chronologically over 8 weeks [3]. We used the total perimeter of newly formed bone adhered to β -TCP as one of the indices of bone formation, and found that the perimeter significantly increased from day 7 to day 28, suggesting that bone formation was enhanced over this period.

There were TRAP-positive and ED1-positive cells around β -TCP at all stages, suggesting that the monocyte-macrophage lineage, including macrophages and osteoclasts, continuously adhered to the surface of the β -TCP and resorbed the material. Although there was no new bone on day 4, osteoblastic differentiation markers such as COL1A1 and osteopontin mRNA were present in the cells around β -TCP. These findings suggest that the bone-forming activity and bioresorption of β -TCP occurred simultaneously on day 4. It has been

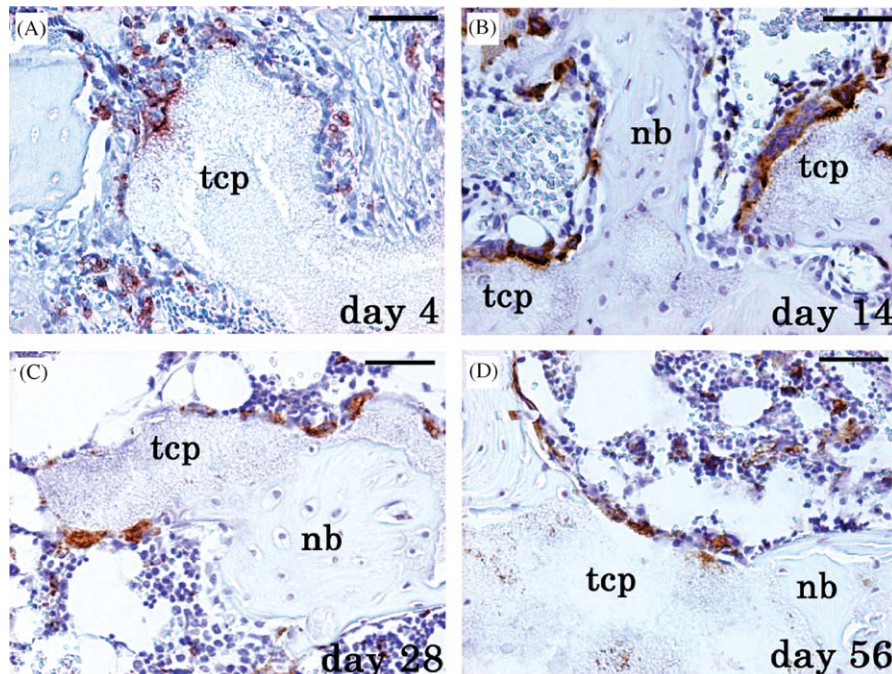


Fig. 4. Immunohistochemistry of the ED1 protein. ED1-positive cells adhered to β -TCP over the whole period. A. Day 4: Most ED1-positive cells between the particles were monocytes. Some multinucleated ED1-positive cells adhered to β -TCP. B. Day 14: Most of the ED1-positive cells were multinucleated. C and D. Days 28 and 56: ED1-positive cells were also detected at the later stages. tcp, tricalcium phosphate; nb, new bone; Bar, A–D, 50 μ m.

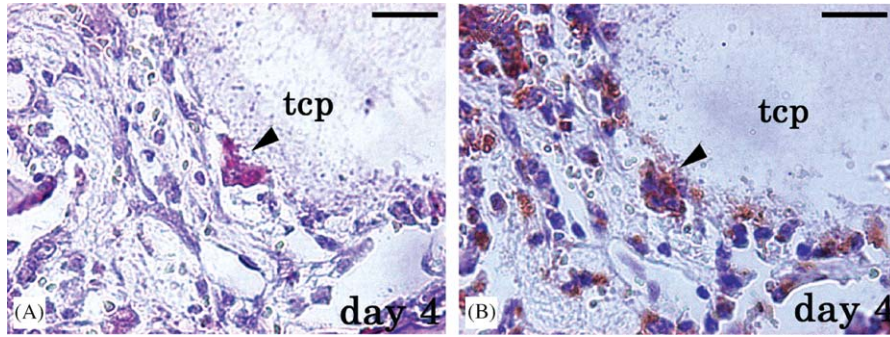


Fig. 5. Serial sections showing TRAP staining and ED1 protein immunohistochemistry on day 4. TRAP-positive multinucleated cells adhered to β -TCP (A) and were also positive for ED1 (B) (black arrow heads). tcp, tricalcium phosphate; Bar, A and B, 25 μ m.

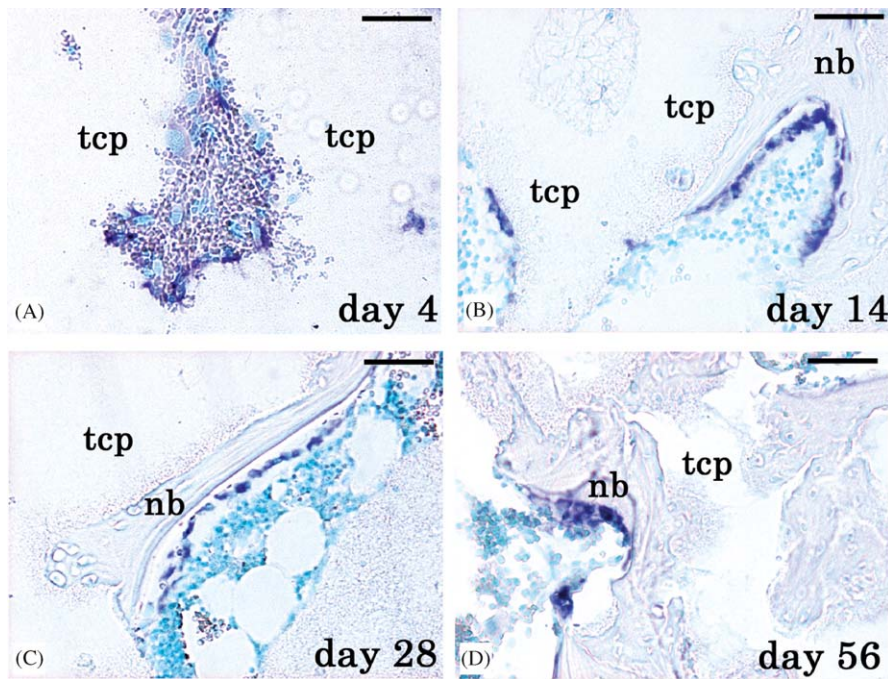


Fig. 6. In situ hybridization of COL1A1 mRNA. A. Day 4: There were some COL1A1 mRNA-positive cells around the β -TCP. B. Day 14: Most COL1A1 mRNA-positive cells were aligned with newly formed bone adhered to β -TCP, and some COL1A1 mRNA-positive cells adhered to β -TCP. C. Day 28: All the COL1A1 mRNA-positive cells were aligned with newly formed bone without signals for COL1A1 mRNA around the β -TCP. D. Day 56: Similar findings on day 28 were observed. tcp, tricalcium phosphate; nb, new bone; Bar, A–D, 50 μ m.

reported that multinucleated giant cells or macrophages adhered to implanted β -TCP in animals, and these cells play a central role in bioresorption of β -TCP [3,10–13]. Multinucleated cells, TRAP-positive cells, or macrophages were in contact with the β -TCP surface from 2 to 4 weeks after implantation, and these cells have been shown to resorb β -TCP, detected by light microscopy or electron microscopy [3,10–13]. In contrast, there are few reports regarding the role of osteoclasts or bioresorptive cells at an early stage of bioresorption of β -TCP. In this study, we detected multinucleated TRAP-positive cells around β -TCP on day 4 after implantation in the rat femora, which was earlier than in the previous reports.

Jarcho assumed that two different biological resorption pathways existed: a solution-mediated process and a cell-mediated process [14]. The appearance of TRAP-positive and ED1-positive cells at an early stage suggests that cell-mediated disintegration of β -TCP plays a central role in the bioresorption of β -TCP.

Osteopontin is a 44 kDa phosphoprotein that is abundant in bone matrix [15]. Immunohistochemical analysis of rat developing bone shows the presence of osteopontin in fibroblast-shaped cells (pre-osteoblasts) between bone trabeculae. They presented not in contact with bony extracellular matrix but with both osteoblasts and osteocytes showing strong staining [16].

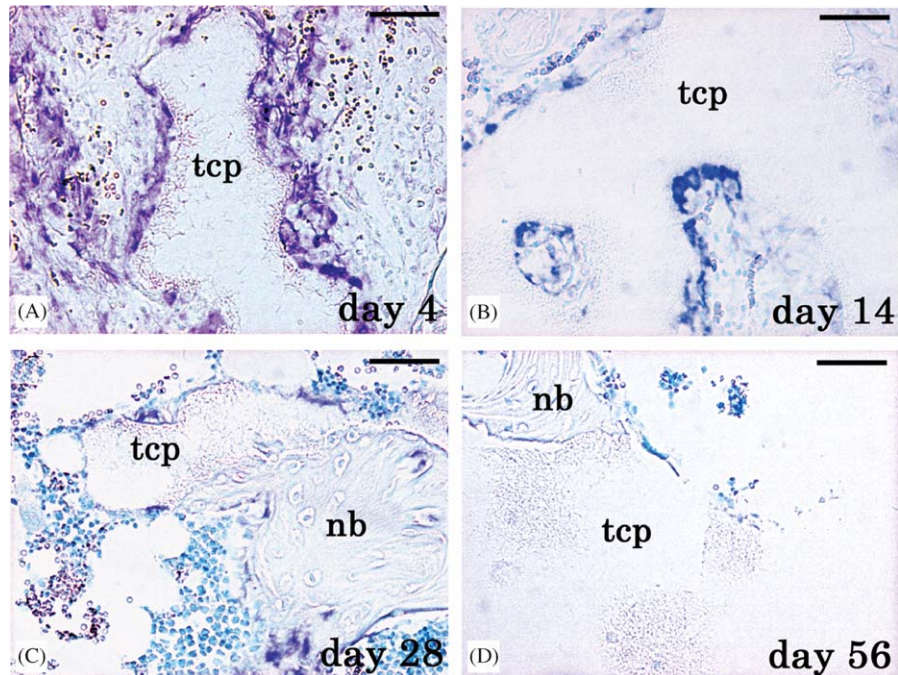


Fig. 7. In situ hybridization of osteopontin mRNA. **A.** Day 4: Osteopontin mRNA-positive cells were abundant around β -TCP, and fibroblast-like cells in bone marrow adjacent to β -TCP were also positive for osteopontin mRNA. **B.** Day 14: Most of the cuboidal-shaped cells around the β -TCP were positive for osteopontin mRNA. **C.** Day 28: There were osteopontin mRNA-positive cells around both the β -TCP and the newly formed bone. **D.** Day 56: there was no signal for osteopontin mRNA around either the β -TCP or the newly formed bone. tcp, tricalcium phosphate; nb, new bone; Bar, **A–D**, 50 μ m.

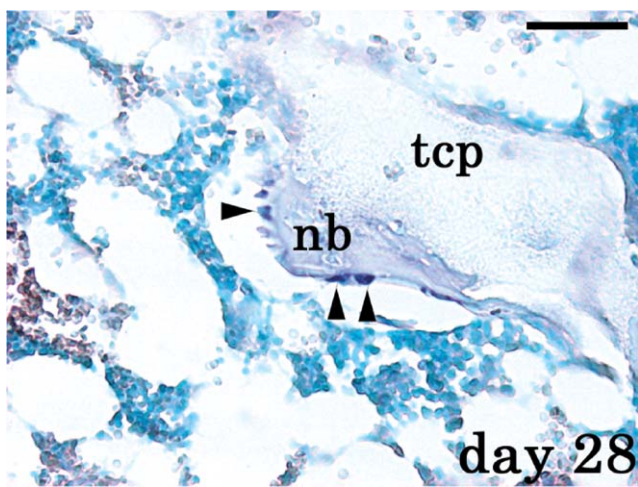


Fig. 8. In situ hybridization of osteocalcin mRNA on day 28. Some osteocalcin mRNA-positive osteoblasts (black arrow heads) were observed on the newly formed bone. However, no osteocalcin mRNA-positive cells on the β -TCP was observed. tcp, tricalcium phosphate; nb, new bone; Bar, 50 μ m.

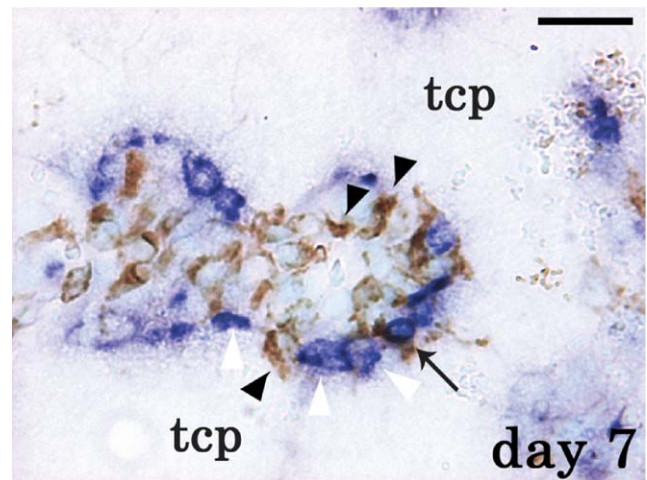


Fig. 9. Double staining using in situ hybridization of osteopontin mRNA and immunohistochemistry of ED1 protein on day 7. Most cells on the β -TCP were singly positive for osteopontin mRNA (white arrow heads) or ED1 (black arrow heads). However, the doubly positive cell for osteopontin mRNA and ED1 protein was detected on the β -TCP (black arrow). tcp, tricalcium phosphate; Bar, 25 μ m.

Osteopontin mRNA exhibits a biphasic pattern of expression during the osteoblast developmental sequence in fetal rat calvaria, with mRNA levels during the period of cell proliferation that are about 25% those observed during the period of mineralization [17,18].

However, it has also been demonstrated that osteopontin mRNA is expressed by osteoclasts [19–22]. Dodds et al. showed that osteopontin mRNA expressed in osteoclasts might facilitate the adhesion of the osteoclast to the bone surface in humans [19]. Merry

et al. detected a high level of osteopontin mRNA expressed in osteoclasts and in a population of mononuclear cells in resorption lacunae in osteophytes of adult human bone [20]. Conner et al. detected osteopontin mRNA expression in osteoclasts at resorption sites within adult human osteophytic bone [21]. Hao et al. detected immunoreactivity for osteopontin in the superficial layer of α -TCP underneath active osteoclasts, following implantation in the rat femoral cortical bone cavity [22].

On the other hand, Ohsawa et al. detected osteopontin mRNA-positive and COL1A1 mRNA-negative round cells using in situ hybridization on days 5 and 7 after implantation of β -TCP in the rat proximal tibiae, and they speculated that these cells were macrophages [1]. Osteopontin is also expressed at sites of inflammation during tissue wound healing or infection [23], and it has been proposed that osteopontin acted as an opsonin, facilitating macrophage adhesion and phagocytosis of particulate mineralized tissue debris [24].

Since it was impossible to distinguish whether osteopontin mRNA-positive cells were osteoblasts, osteoclasts, or another cell type, we performed the double staining using in situ hybridization of osteopontin mRNA and immunohistochemistry of the ED1 protein. Most mononuclear and multinucleated cells around β -TCP were single positive for osteopontin mRNA or ED1 protein on days 4 and 7, and only a few multinucleated cells were doubly positive for both osteopontin mRNA and ED1 protein. Bone formation was observed on day 7. From these findings, we speculate that a part of the singly osteopontin mRNA-positive mononuclear cells around β -TCP were undifferentiated osteoblasts or macrophages and that the singly osteopontin mRNA-positive multinucleated cells were osteoclasts. Furthermore, we speculate that mononuclear cells with the singly ED1-positive belong to the mononuclear phagocyte system such as macrophages, and that the multinucleated cells with doubly positive for osteopontin mRNA as well as ED1 are osteoclasts. We confirmed that many of the ED1-positive cells were also positive for TRAP staining in the serial sections, suggesting these cells are osteoclasts.

Only a few in situ hybridization studies of osteoblast differentiation markers after implantation of β -TCP have been performed [1,10,25]. Neo et al. showed that osteoblasts, which were strongly positive for COL1A1 mRNA, colonized on the surface of β -TCP on day 7 after implantation in the distal femora epiphysis of rabbits [25]. These authors also showed that most COL1A1 mRNA-positive cells existed between β -TCP beads, rather than adhered to β -TCP, on days 5, 7, and 14 after implantation in rat tibiae [10]. Ohsawa et al. demonstrated that COL1A1 mRNA-positive osteoblasts were observed around implanted β -TCP on day 3 after implantation, and that both osteopontin and osteocalcin

mRNA-positive osteoblasts were identified around β -TCP by day 7, following implantation in rat tibiae [1]. The β -TCP used by Neo and Ohsawa et al. [1,10] had little macropores and 1.5% porosity. It is quite different from the highly purified β -TCP used in this study in terms of the process of manufacturing, the porosity, and the character of the pore. We suggest that these differences cause different expression patterns of osteoblastic lineage markers such as COL1A1, osteopontin, and osteocalcin mRNA in osteoblasts.

In this study, osteoblasts around the β -TCP implant were positive for COL1A1 mRNA on days 4, 7 and 14, positive for osteopontin mRNA on days 4, 7, 14 and 28, and negative for osteocalcin mRNA over the entire period. In contrast, there were osteocalcin mRNA-positive cells around the newly formed bone only on day 28, although the number of these cells was very low. Okumura et al. showed positive signals for osteocalcin mRNA in the cytoplasmic areas of cuboidal-shaped osteoblasts on a hydroxyapatite (HA) surface 3 weeks after postsubcutaneous marrow/HA implantation in rat [26]. Osteocalcin is responsible for calcium ion binding and is believed to be a marker of the late stage of osteoblastic differentiation [27]. Our findings suggest that most of the osteoblasts around β -TCP have undifferentiated characteristics.

5. Conclusion

We found that highly purified β -TCP provided an early bone conduction, followed by bioresorption of β -TCP and the replacement of large parts of the β -TCP with newly formed bone. We further showed that osteoblasts, osteoclasts, and mononuclear macrophages adhered to β -TCP on day 4, and that ED1-positive and TRAP-positive cells which adhered to β -TCP continuously resorb β -TCP implant at all stages. Collectively, these results suggest that highly purified β -TCP is a biocompatible, resorbable bioactive ceramic.

Acknowledgements

The authors thank Yoshiaki Tanaka (Division of Orthopedic Surgery, Department of Regenerative and Transplant Medicine, Niigata University Graduate School of Medical and Dental Sciences) for his technical assistance.

References

- [1] Ohsawa K, Neo M, Matsuoka H, Akiyama H, Ito H, Kohno H, Nakamura T. The expression of bone matrix protein mRNAs around beta-TCP particles implanted into bone. *J Biomed Mater Res* 2000;52:460–6.

- [2] Ozawa M, Tanaka K, Morikawa S, Chazono M, Fujii K. Clinical study of the pure β -tricalcium phosphate—reports of 167 cases. *J East Jpn Orthop Traumatol* 2000;12:409–13.
- [3] Chazono M, Tanaka T, Komaki H, Fujii K. Bone formation and bioresorption after implantation of injectable β -tricalcium phosphate granules-hyaluronate complex in rabbit bone defects. *J Biomed Mater Res* 2004;70A:542–9.
- [4] Burstone MS. Histochemical demonstration of acid phosphatase with naphthol AS-phosphate. *J Nat Cancer Int* 1958;21:523–39.
- [5] Amizuka N, Yamada M, Watanabe J, Hoshi K, Fukushi M, Oda K, Ikehara Y, Ozawa H. Morphological examination of bone synthesis via direct administration of basic fibroblast growth factor into rat bone marrow. *Microsc Res Tech* 1998;41:313–22.
- [6] Yamagiwa H, Tokunaga K, Hayami T, Hatano H, Uchida M, Endo N, Takahashi HE. Expression of metalloproteinase-13 (Collagenase-3) is induced during fracture healing in mice. *Bone* 1999;25:197–203.
- [7] Hayami T, Endo N, Tokunaga K, Yamagiwa H, Hatano H, Uchida M, Takahashi HE. Spatiotemporal change of rat collagenase (MMP-13) mRNA expression in the development of rat femoral neck. *J Bone Miner Metab* 2000;18:185–93.
- [8] Damoiseaux JGMC, Döpp EA, Calame W, Chao D, Macpherson GG, Dijkstra CD. Rat macrophage lysosomal membrane antigen recognized by monoclonal antibody ED1. *Immunology* 1994;83:140–7.
- [9] Dijkstra CD, Döpp EA, Joling P, Kraal G. The heterogeneity of mononuclear phagocytes in lymphoid organs: distinct macrophage subpopulations in the rat recognized by monoclonal antibodies ED1, ED2, and ED3. *Immunology* 1985;54:589.
- [10] Neo M, Herbst H, Voigt CF, Gross UM. Temporal and spatial of osteoblast activation following implantation of β -TCP particles into bone. *J Biomed Mater Res* 1998;39:71–6.
- [11] Wada T, Hara K, Ozawa H. Ultrastructural and histochemical study of β -tricalcium phosphate resorbing cells in periodontium of dogs. *J Periodont Res* 1989;24:391–401.
- [12] Renooij W, Hoogendoorn HA, Visser WJ, Lentferink RHF, Schmitz MGJ, Ieperen HV, Oldenberg SJ, Janssen WM, Akkermans LMA, Wittebol P. Bioresorption of ceramic strontium-85-labeled calcium phosphate implants in dog femora: a pilot study to quantitate bioresorption of ceramic implants of hydroxyapatite and tricalcium orthophosphate in vivo. *Clin Orthop* 1985;197:272–85.
- [13] Egli PS, Muller W, Shenk RK. Porous hydroxyapatite and tricalcium phosphate cylinders with two different pore size ranges implanted in cancellous bone in rabbits. *Clin Orthop* 1988;232:127–38.
- [14] Jarcho M. Calcium phosphate ceramics as hard tissue prosthesis. *Clin Orthop* 1981;157:259–78.
- [15] Yoon K, Buenaga R, Rodan GA. Tissue specificity and developmental expression of rat osteopontin. *Biochem Biophys Res Commun* 1987;148:1129–36.
- [16] Mark MP, Prince CW, Oosawa T, Gay S, Bronckers AL, Butler WT. Immunohistochemical demonstration of a 44-KD phosphoprotein developing rat bones. *J Histochem Cytochem* 1987;35:707–15.
- [17] Stein GS, Lian JB, Owen TA. Relationship of cell growth to the regulation of tissue-specific gene expression during osteoblast differentiation. *FASEB J* 1990;4:3111–23.
- [18] Owen TA, Aronow M, Shalhoub V, Barone LM, Willaming L, Tassinari MS, Kennedy MB, Pockwinse S, Lian JB, Stein GS. Progressive development of the rat osteoblast phenotype in vitro: reciprocal relationships in expression of genes associated with osteoblast proliferation and differentiation during formation of the bone extracellular matrix. *J Cell Physiol* 1989;143:420–30.
- [19] Dodds RA, Corner JR, James IE, Rykaczewski EL, Appenbaum E, Dul E, Gowen M. Human osteoclasts, not osteoblasts, deposit OPN onto resorption surfaces, an in vitro and ex vivo study of remodeling bone. *J Bone Miner Res* 1995;10:1666–80.
- [20] Merry K, Dodds R, Littlewood A, Gowen M. Expression of osteopontin mRNA by osteoclasts and osteoblasts in modeling adult human bone. *J Cell Sci* 1993;104:1013–20.
- [21] Conner JR, Dodds RA, James IE, Gowen M. Human osteoclast and giant cell differentiation: the apparent switch from non-specific esterase to tartrate resistant acid phosphatase activity coincides with in situ expression of osteopontin mRNA. *J Histochem Cytochem* 1995;43:1193–201.
- [22] Hao H, Amizuka N, Oda K, Fujii N, Ohnishi H, Okada A, Nomura S, Maeda T. A histological evaluation on self-setting α -tricalcium phosphate applied in the rat bone cavity. *Biomaterials* 2004;25:431–42.
- [23] Denhardt DT, Noda M. Osteopontin expression and function: role in bone remodeling. *J Cell Biochem Suppl* 1998;30/31:92–102.
- [24] McKee MD, Nanci A. Secretion of osteopontin by macrophages and its accumulation at tissue surfaces during wound healing in mineralized tissues: a potential requirement for macrophage adhesion and phagocytosis. *Anat Rec* 1996;245:394–409.
- [25] Neo M, Voigt CF, Herbst H, Gross UM. Analysis of osteoblast activity at biomaterial-bone interfaces by in situ hybridization. *J Biomed Mater Res* 1996;30:485–92.
- [26] Okumura M, Ohgushi H, Dohi Y, Katsuda T, Tamai S, Koerten HK, Tabata S. Osteoblastic phenotype expression on the surface of hydroxyapatite ceramics. *J Biomed Mater Res* 1997;37:122–9.
- [27] Wang C, Duan Y, Markovic B, Barbara J, Howlett CR, Zhang X, Zreiqat H. Proliferation and bone-related gene expression of osteoblasts grown on hydroxyapatite ceramics sintered at different temperature. *Biomaterials* 2004;25:2949–56.